Wavelength-scanning digital interference holography for optical section imaging

M. K. Kim

Department of Physics, University of South Florida, Tampa, Florida 33620

Received August 16, 1999

We propose and experimentally demonstrate a simple digital holographic method that allows reconstruction of three-dimensional object images with a narrow depth of focus or axial resolution. A number of holograms are optically generated by use of different wavelengths spaced at regular intervals. The holograms are recorded on a digital camera and reconstructed numerically. Multiwavelength interference of the holograms results in images of the contour plane whose thickness can be made arbitrarily narrow. Objects at different distances from the hologram plane are imaged clearly and independently, with complete suppression of the out-of-focus images. The technique is available only in digital holography and should have useful applications in holographic microscopy. © 1999 Optical Society of America

OCIS codes: 090.1760, 090.4220, 110.6880.

By recording not only the intensity but also the phase information of a light wave arriving at a recording medium, holography allows three-dimensional visualization of real objects and gives rise to a host of metrological techniques and optical information processing applications.[1] With the advance of computer and electronic imaging technology, it is now very practical and often advantageous to replace portions of holographic procedures with electronic processes. Thus holographic interference patterns can be calculated from mathematically defined models of a three-dimensional scene.[2,3] These patterns are referred to as computer-generated holograms, which are then recreated optically by laser illumination of the hard copy of a computer-generated hologram. Complimentarily, in digital or computer-reconstructed holograms the optical interference pattern between the object and the reference waves is recorded by an electronic camera and stored in a computer, and the holographic image is recreated on the computer by numerical calculation.[4] In either computer-generated or computer-reconstructed holograms, the numerical calculation basically imitates the optical diffraction process as the light wave propagates from the object to the hologram and to the image plane, by use of Fresnel diffraction theory or Huygens wavelet theory.[5] The computational load can be minimized by segmentation of holograms and by horizontal-only parallax.[6,7] The phase information of the light wave is available directly from the numerical reconstruction and greatly simplifies interferometric deformation analysis.[8–10]

In this Letter we propose a simple digital holographic technique that allows reconstruction of three-dimensional object images with a narrow axial resolution. As is well known, interference of two holograms recorded at two different wavelengths results in a contour interferogram, with the axial distance between the contour planes inversely proportional to the difference in wavelengths. In computer-reconstructed holography, unlike in conventional holography, the reconstruction of each hologram is done with the corresponding wavelength that was actually used in the recording process. Therefore it is possible to extend the process to recording and reconstruction of many holograms without introducing any wavelength mismatch. If a number of regularly spaced wavelengths are used for recording and reconstruction, then the peaks of the cosine squared intensity variation of two-wavelength interference become sharper and narrower, as when a number of cosines with regularly spaced frequencies are added. The present work has been motivated by a practical problem in microscopy, in which the axial magnification is proportional to the square of the transverse magnification. Even at moderate magnification, it is difficult to bring the entire microscopic object into focus, whereas the out-of-focus portions of the object image contribute to blurring and noise of the focal-plane image. Confocal scanning microscopy addresses this problem very successfully,[11] although the requirements of stability and precision of lengthy mechanical scanning can be quite significant. A hologram, of course, has perceived depth and axial resolution, but determination of axial location in particle analysis, for example, depends only on the focusing of the image as the depth is varied,[12,13] and out-of-focus blurring presents the same problem as in conventional microscopy. Several authors have proposed holographic depth resolution by use of time-gated interference of short pulses or phase-sensitive detection of a time-modulated signal.[14] The technique proposed here involves no mechanical motion, and wavelength scanning and multiple exposure can be electronically automated for speed and stability.

To outline the proposed technique we start by stating that one of the diffracted fields of a hologram, E_i, recreates an exact replica of the object wave, E_o. So we consider an object point P located at (x_o, y_o, z_o) that emits a Huygens spherical wavelet proportional to $A(\mathrm{P})\exp(ikr_P)$ measured at an arbitrary point Q located at (x, y, z), where $r_\mathrm{P} = |\mathbf{r}_\mathrm{P} - \mathbf{r}_Q|$ is the distance between P and Q, and we neglect the $1/r$ dependence of the amplitude. The wave propagates in the general z direction. The factor $A(\mathrm{P})$ represents the field amplitude and phase at the object point. For an extended object, the field at Q is proportional to the

0146-9592/99/231693-03$15.00/0

above-described wavelet field integrated over all the points on the object:

$$E_k(\mathrm{Q}) \sim \int_{\mathrm{P}} \mathrm{d}^3\mathbf{r}_{\mathrm{P}}\, A(\mathrm{P})\exp(ikr_{\mathrm{P}})\,. \tag{1}$$

The factor $\exp(ikr_{\mathrm{P}})$ represents the propagation and diffraction of the object wave. Now suppose that a number of copies of the electric field are generated by variation of the wave numbers k (or wavelengths λ), with all other conditions of object and illumination remaining the same. Then the resultant field at Q is

$$\begin{aligned} E(\mathrm{Q}) &\sim \sum_k \int_{\mathrm{P}} \mathrm{d}^3\mathbf{r}_{\mathrm{P}}\, A(\mathrm{P})\exp(ikr_{\mathrm{P}}) \\ &\sim \int_{\mathrm{P}} \mathrm{d}^3\mathbf{r}_{\mathrm{P}}\, A(\mathrm{P})\delta(\mathbf{r}_{\mathrm{P}} - \mathbf{r}_{\mathrm{Q}}) \\ &\sim A(\mathrm{Q})\,. \end{aligned} \tag{2}$$

That is, for a large enough number of wave numbers k, the resultant field is proportional to the field at the object and is nonzero only at object points. In practice, if one uses a finite number N of wavelengths at regular intervals of $\Delta\lambda$ (with corresponding intervals of frequencies Δf), then the object image $A(\mathrm{P})$ repeats itself at axial distances $\Lambda = \lambda^2/\Delta\lambda = c/\Delta f$, with axial resolution $\delta = \Lambda/N$. By use of appropriate values of $\Delta\lambda$ and N, the contour-plane distance Λ can be matched to the axial extent of the object, and δ, to the desired level of axial resolution. In fact, relation (2) can also be interpreted as a Fourier transform in r_{P} and is the basis of the method described as laser radar.[15]

A proof-of-principle experiment was performed by use of the apparatus depicted in Fig. 1. A ring dye laser (RDL) provides a 595.0-nm laser field of ~50-mW power, with a linewidth of ~50 MHz. The laser beam is expanded with a microscope objective (MO) to 20-mm diameter (lens L1) and divided into three parts by beam splitters (BS's). One of these beams provides the planar reference beam (REF), and the other two constitute the object beam. The object consists of two transparent targets attached to the backreflecting mirrors (M's) in separate optical arms, allowing us to avoid obstruction of one object by the other in the same optical path. One target, OBJ1, is a checkerboard pattern with a 2.5-mm grid size, and the other target, OBJ2, is a transparent letter A that fits inside an opaque square with 13-mm sides. The object and the reference beams are combined in a Michelson interferometer arrangement and sent to a translucent Mylar screen, S. The object distances to the screen are approximately 149 and 167 cm for OBJ1 and OBJ2, respectively. The interference pattern on the screen is imaged by a digital camera (DC; Kodak DC 120) through another lens, L2, for adjustment of focus and magnification. The camera has 960 × 1280 pixels, with a 10 μm × 10 μm pixel size. All the calculations presented here use 256 × 256 pixel images of screen area 13 mm × 13 mm, so that the effective pixel resolution on the screen is 51 μm. We set the corresponding minimum distance for the object as 1.1 m to accommodate interference between rays emanating from the two ends of a 13-mm object. For each hologram we also image the reference and the object beams separately so that these images can be subtracted before reconstruction, and the resulting images do not contain zero-order terms. We do not try to eliminate the conjugate image. The process is repeated for as many as 11 laser frequencies spaced 1.0 GHz apart, so the axial period Λ of the resultant hologram images is 30 cm and the axial resolution δ is 3.0 cm. For reconstruction of images we use a MatLab program that encodes the Fresnel diffraction, which is equivalent to relation (1) with appropriate approximation

$$\begin{aligned} E(x,y;z) = \exp\!\left[\frac{ik}{2z}(x^2+y^2)\right] \\ \times F\{E_0(x_0,y_0)S(x_0,y_0;z)\}[\kappa_x,\kappa_y], \end{aligned} \tag{3}$$

where

$$S(x,y;z) = -\frac{ik}{z}\exp\!\left[ikz + \frac{ik}{2z}(x^2+y^2)\right], \tag{4}$$

$\kappa_x = kx/z$, $\kappa_y = ky/z$, and $F\{f\}[\kappa]$ stands for the Fourier transform of f with respect to the variable κ.

Figure 2(a) shows the images of the interference hologram (H) between the reference (R) and the object (O) beams, and Fig. 2(b) shows the subtracted image, E = H − R − O. The holographic image in Fig. 2(c) of a single object, and a single wavelength, is reconstructed at $z_i = 149$ cm and shows the typical resolution and quality of the reconstructed images (z_o and z_i are the object and image distances, respectively, measured from the screen.) The remaining fringe pattern inside the squares is due to the out-of-focus twin image.

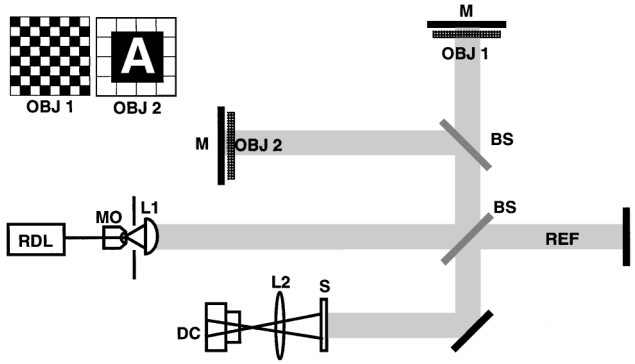

Fig. 1. Apparatus for wavelength-scanning digital interference holography. See text for details.

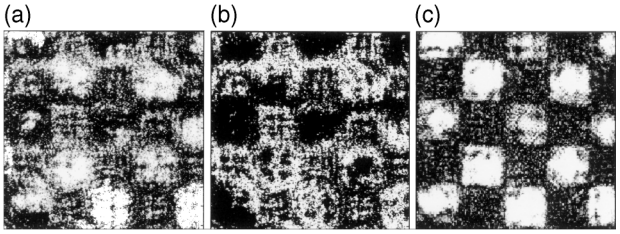

Fig. 2. Reconstruction of the image of a single object (OBJ1) by use of a single wavelength: (a) interference between reference and object, (b) intensity pattern of (a) minus those of the reference and object beams, (c) numerically reconstructed image at $z_i = z_o = 149$ cm.

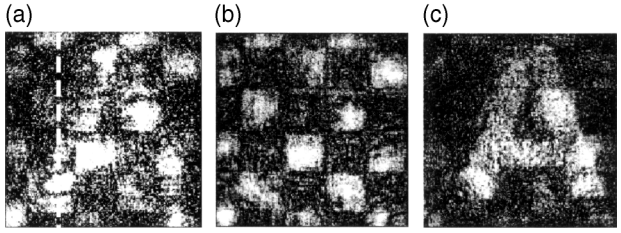

Fig. 3. Reconstruction of the images of two objects (OBJ1 and OBJ2) by use of (a) a single wavelength at $z_i = z_{o2} =$ 165 cm (the image at 149 cm is quite indistinguishable from this image), (b) 11 holograms at $z_i = z_{o1} = 149$ cm, or (c) 11 holograms at $z_i = z_{o2} = 165$ cm.

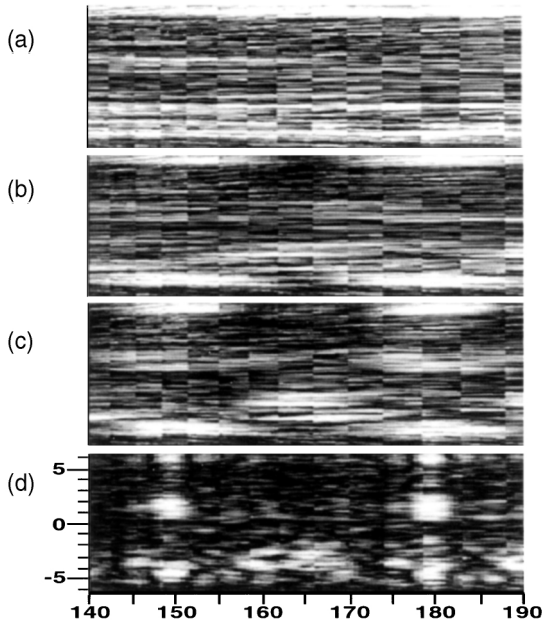

Fig. 4. Reconstructed image patterns as functions of image distance. The horizontal axis is z_i (in centimeters) and the vertical axis is a slice of the reconstructed image (in millimeters) along the dotted line in Fig. 3(a): (a) single wavelength or frequency; (b) combination of two holograms at relative frequencies, 0.0 and 1.0 GHz; (c) three relative frequencies, 0.0, 1.0, and 2.0 GHz; (d) 11 relative frequencies, 0.0, 1.0, 2.0, ..., 10.0 GHz.

Figure 3(a) shows the reconstructed image with both objects OBJ1 and OBJ2 illuminated, with a single wavelength, at $z_i = 165$ cm. The image is essentially indistinguishable if $z_i = 149$ cm, although it is possible to discern slight differences in the sharpness of focus. On the other hand, if we add holograms of 11 wavelengths at 1.0-GHz intervals, the results are as shown in Figs. 3(b) and 3(c). Each of the images contains only OBJ1 or OBJ2, and the out-of-focus images are clearly suppressed. The axial resolution determined by focal sharpness alone is at least 20–30 cm, as can be seen from Fig. 4(a), in which the vertical axis is a slice of the reconstructed image along the dotted vertical line in Fig. 3(a) and the horizontal axis is the image distance z_i from 140 to 190 cm. In Fig. 4(b) two holograms with frequency separation of 1.0 GHz are combined, and the figure shows the expected cosine squared modulation, with a period of 30 cm. In Fig. 4(c), three relative frequencies of 0.0, 1.0, and 2.0 GHz are combined, and the narrowing of the interference maxima is evident. Also note that the images of OBJ1 and OBJ2 focus at different z_i locations: The three bright areas near $z_i = 150$ cm (and also at 180 cm) are the three bright squares of OBJ1's checkerboard, and the bright patch near $y = -3.0$ mm, $z_i =$ 165 cm corresponds to the lower left hand of OBJ2's letter A. Carrying the process further, 11 holograms with frequencies 0.0, 1.0, 2.0, ..., 10.0 GHz are combined in Fig. 4(d), which results in axial resolution of ~3 cm, as expected.

The experiment thus demonstrates the feasibility of using multiwavelength interference of computer-reconstructed holograms for high axial resolution of three-dimensional images. The apparatus is very simple and amenable to electronic automation without mechanical moving parts. Even with the less-than-optimal laser and imaging systems employed here, the theoretically predicted axial resolution is easily achieved. The main sources of imperfection in Fig. 4, for example, were the mode hop and drift of the nonstabilized laser frequency.

The author thanks N. Djeu for the use of the ring dye laser and for useful discussions; his e-mail address is myungkim@chuma.cas.usf.edu.

References

1. P. Hariharan, *Optical Holography* (Cambridge U. Press, Cambridge, 1996).
2. S. Trester, Am. J. Phys. **64,** 472 (1996).
3. V. N. Karnaukhov, N. S. Merzlyakov, M. G. Mozerov, L. P. Yaroslavsky, L. I. Dimitrov, and E. Wenger, Proc. SPIE **2363,** 164 (1995).
4. U. Schnars and W. P. O. Jüptner, Laser Optoelektron. **26,** 40 (1994) [in German]; U. Schnars, M. Thomas, and W. P. Jüptner, Opt. Eng. **35,** 977 (1996).
5. T. M. Kreis, M. Adams, and W. P. O. Jüptner, Proc. SPIE **3096,** 224 (1997).
6. V. N. Karnaukhov, N. S. Merzlyakov, M. G. Mozerov, L. I. Dimitrov, and E. Wenger, Opt. Lasers Eng. **29,** 361 (1998).
7. H. G. Yang, C. Y. Ryu, and E. S. Kim, J. Korea Inst. Electron. Eng. D **35,** 76 (1998) [in Korean]; H. Yang, K. T. Kim, J. H. Kim, and E. S. Kim, Proc. SPIE **3389,** 169 (1998).
8. S. Seebacher, W. Osten, and W. Jüptner, Proc. SPIE **3479,** 104 (1998); T. M. Kreis, W. P. O. Jeuptner, and J. Geldmacher, Proc. SPIE **3407,** 169 (1998).
9. E. Cuche, F. Bevilacqua, and C. Depeursinge, Opt. Lett. **24,** 291 (1999).
10. G. C. Brown and R. J. Pryputniewicz, Opt. Eng. **37,** 1398 (1998).
11. C. J. R. Sheppard and D. M. Shotton, *Confocal Laser Scanning Microscopy* (Springer, New York, 1997).
12. T. Zhang and I. Yamaguchi, Opt. Lett. **23,** 1221 (1998).
13. T. C. Poon, K. B. Doh, and B. W. Schilling, Opt. Eng. **34,** 1338 (1995). This paper presents a novel method of depth measurement by use of a time-dependent Fresnel zone pattern.
14. S. C. W. Hyde, N. P. Barry, R. Jones, J. C. Dainty, and P. M. W. French, Opt. Lett. **20,** 2330 (1995); T. C. Poon, K. B. Doh, and B. W. Schilling, Opt. Eng. **34,** 1338 (1995).
15. J. C. Marron and K. S. Schroeder, Appl. Opt. **31,** 255 (1992); Opt. Lett. **18,** 385 (1993).